

On the Emulation of Natural Movements by Humanoid Robots

Magnus J. E. Richardson^{1,2} and Tamar Flash²

¹ Laboratoire de Physique Statistique, Ecole Normale Supérieure,
24 rue Lhomond 75231, Paris Cedex 05, France
Magnus.Richardson@lps.ens.fr

² Department of Applied Mathematics, The Weizmann Institute of Science,
Rehovot, 76200, Israel.
tamar@wisdom.weizmann.ac.il

Abstract. Proposed movement-planning strategies from the field of human motor control are examined for possible emulation by robotic systems. There are many hypotheses for human arm-movement planning, often specialized to particular experimental tasks. However, motion planning algorithms for humanoid robots should be as widely applicable as possible, whilst at the same time being computationally simple. A mathematical analysis of current human motor-control strategies is therefore needed, with the aim of simplification and unification of theories. In this paper, such a unification is demonstrated for two movement-planning strategies with quite different underlying principles. To be specific, the predictions of the empirical two-thirds power law will be derived mathematically from a smoothness cost-function approach. Two figural shapes will be analyzed in the context of drawing: the ellipse and the cloverleaf. The power-law exponent predicted from the cost function will be shown to be $\beta = 0.33$ and $\beta = 0.36$ in excellent agreement with experimental results. Though these theories are known only to describe a sub-set of possible movements, the method used is illustrative of the approach that will be needed to obtain simple algorithms for the full seven-degrees-of-freedom anthropomorphic arm.

1 Introduction

There has been a rich exchange of ideas between the fields of biological motor-control research and robotics [1]. The planning strategies used by the central nervous system (CNS) are unrivaled in their versatility and one of the goals in the study of the human motor system has been to identify these efficient algorithms for use in robotics. However, it is not clear that it would be always advantageous for humanoid robots to use the same planning strategies for movements that humans use. It is widely assumed that humans perform movements that are optimal in some sense, but what is optimal for the human arm and CNS might well be sub-optimal or overly restrictive for the robotic arm and its controller. For example, it was suggested recently that humans plan movements that minimize the transmission of error, from the noisy biological components, to the achievement of the motor task [2, 3]. Though this hypothesis predicted trajectories in excellent agreement with experiment, the underlying principle does not translate well to robots. In digital systems noise is not really an issue, and hence movements based on this hypothesis would indeed be rather restrictive.

One of the main reasons for embarking on the difficult project of building humanoids is to produce robots that can perform in unaltered human environments. This means that humanoids must (when necessary) be able to move and manipulate objects in the same fashion as humans. For this to be possible it must first be decided exactly how humans move. A huge amount of research has already been performed on human motor planning, and as is described below, many different theories exist. All of them capture some aspect of natural movement, but as yet there are no simple and general prescriptions. Fortunately, to produce human-like movement all that is necessary is that versatile and efficient algorithms be found that reproduce the motion seen in experiment, i.e. a phenomenological approach is sufficient. This at least bypasses some of the difficult arguments concerning what is the apparent behavior of the arm, and what planning processes are in fact occurring in the CNS.

The aim in this paper is to examine two apparently different human motor-control hypotheses, and show that one of them can produce the predictions of the other. Specifically, the minimum-jerk cost function will be used to derive the exponents seen in the empirical two-thirds power law, mathematically. It should be noted that here the approach does not need any input from experiment to fit curves, unlike in [4] where kinematic information was included at certain via points on the curves. This result of this present paper, in conjunction with a wealth of successful predictions of other experimental tasks [5, 6] implies this simple cost function provides a computationally efficient and versatile description for a large sub-set of motor tasks: those of drawing, writing and pointing in the plane. This is, of course, a rather modest step towards the goal of finding simple set of algorithms for the full seven-degrees-of-freedom arm moving in three dimensions. Before this can be done, much more experimentation

must be undertaken to characterize these aspects of human motion. Nevertheless, a detailed mathematical analysis of the similarities and differences between human motor-control strategies is a necessity for the field of humanoid robotics.

In the rest of this section, some current formulations of human motor-control strategies will be reviewed, in particular the two-thirds power law and minimum-jerk model. In the following section it will be demonstrated how the exponent of the power law can be predicted from the minimum-jerk cost function for shapes that are similar to circles. The result is quite general, but specific examples are given for the frequently studied experimental tasks of ellipse drawing, as well as the more interesting case of the cloverleaf. The paper ends with a summary of extensions to this work and what might be needed for a full model of human arm movement.

1.1 Theories of Human Motor Control

There are no direct experimental means available to obtain the algorithms used by the CNS to plan movements. The experimental approach has been to treat the moving human as a “black-box”, which involves setting simple motor tasks for human subjects and recording the generated arm trajectories. By examining the invariances and qualities of the recorded motion it is hoped that some general strategies of motor planning can be inferred. Because of the variation between test subjects and the tendency of the subjects to alter strategies depending on the task [7], there are a number of competing hypotheses in the literature, each backed up by experimental evidence. For example, it has been proposed that the CNS plans in the coordinates system of the joint angles [8], or in the coordinates of the hand’s position [5] and more recently that the movements planned are robust against the inherent errors in the motor system [3]. Each of these theories is expressed in the form of a cost function of the movement trajectory, with the prediction of the theory being the trajectory that minimizes the corresponding cost. In most cases the approach is numerical, due to the complexity of the cost function, though some analytic results exist [5]. Because the cost is a function of the whole trajectory it can be called a *global* minimization. Contrary to these are the motor planning strategies that are functions of *local* geometric features. An example is the well studied two-thirds power law [9–14] that has been used to predict velocity profiles from local curvature relations. Despite the apparent difference in the underlying principles for these local and global theories, their predictions will be shown to be remarkably similar. The two motor-control hypothesis that will be analyzed in this paper are now defined.

The Two-Thirds Power Law It has been long known that the velocity v of drawing movements decreases at points of high curvature κ . More recently [12] this phenomena was cast in mathematical form

$$v = g \kappa^{-\beta} \quad (1)$$

where the accepted value of the exponent β is $1/3$. The factor g is known as the gain factor and is set by the tempo of the movement. For more complex movements this gain factor varies in a piece-wise fashion. However, in this paper only shapes that experimentally have a constant g , i.e. a single segment on $\log \kappa$ versus $\log v$ plot will be examined. Incidentally, the law (1) was originally drafted in terms of angular velocity, and hence the anachronistic name *two-thirds* power law. Most experimental work on the examination of this law was performed on the periodic tracing of simple figural patterns, principally the ellipse. For this shape, the value of $\beta = 1/3$ implies simple harmonic motion and because of this the theory has been criticized as being trivial [13]. However, developmental studies have shown that children of different ages draw ellipses with an age dependent exponent [10]. Also, experiments on other shapes, for which harmonic solutions do not exist, also suggest a power-law relation though sometimes with a different exponent [10] or with a variable gain factor [14]. All of which is evidence that the velocity-curvature relation as written above is robust, though the exponent is not necessarily always $1/3$.

The Minimum-Jerk Cost Function The experimental examination of reaching movements identified a number of pseudo-invariants. These comprised invariance under rotation, translation and scaling in time or amplitude. The velocity trajectories measured were also smooth. Taken together these experimental facts lead to the postulation [5] of the following cost function

$$C_n = \int_0^T dt \left(\left(\frac{d^3 x}{dt^3} \right)^2 + \left(\frac{d^3 y}{dt^3} \right)^2 \right) \quad (2)$$

where T is the duration of the movement and x and y are the coordinates of the hand. The cost function can be used for obtaining the full trajectory, i.e. the path as well as the time profile. Here however, similarly to [6], it will

be assumed that the path is given in terms of a shape that should be drawn, and hence it is only the velocity profile that will be derived.

Now the models have been defined, the mathematical method for deriving the exponent of the power law (1) from the cost function (2) will be explained.

2 Basic Mathematics for Periodic Drawing Movements

The motor tasks to be examined are continuous, repeated drawing movements of simple figural forms. Much work has been performed experimentally on such movements with most experiments consisting of subjects seated at a table and asked to trace around a given template, with the velocity profile measured digitally. The period of the movement can be fixed either externally using a metronome, or can be spontaneously chosen by the subject. In this section, the mathematical method that will be used to obtain the theoretical predictions for the exponent β will be described. The method is simply to insert the two-thirds power law form into the cost function, but with the exponent kept as a variable to be obtained through minimization. In this way a general form for β , as predicted by the minimization of jerk, can be found. However, an exact calculation is not possible due to the mathematical complexity of the problem. Perturbation theory is therefore used to obtain the exponents at the desired level of approximation.

2.1 The Perturbative Approach

The first step is to re-write the cost function (2) in terms of velocity and curvature. This step can be done conveniently by using Frenet's relations [6]. The result is

$$C = \int_0^L \frac{ds}{v} \left((v^2 v'' + v(v')^2 - \kappa^2 v^3)^2 + (3v'v^2\kappa + v^3\kappa')^2 \right) \quad (3)$$

where s is the arc-length, L is the circumference of the path and in this equation the notation X' means X differentiated with respect to arc-length. Normally, to obtain the velocity profile it would be necessary to functionally minimize this cost with respect to the velocity v . This is rarely possible analytically, and the usual approach is numerical [4, 6]. However, in this case analytic results will be found, by substituting the power law form for v into the cost function and minimizing with respect to β .

The first step is to fix the gain factor g which is done by setting the restriction that all trajectories have the same period

$$\int_0^L \frac{ds}{v} = T.$$

This gives the following form for the gain factor

$$g = \int_0^{2\pi} d\theta \xi \kappa^\beta \quad \text{where } \xi = \frac{ds}{d\theta}$$

where from now on the scaling choice has been made that $T = L = 1$. This is merely a choice of units of time and length, and does not affect the generality of any of the following results. It should be noted that there are two dependencies on β : in the gain factor g and also in the form $\kappa^{-\beta}$

$$v = \left(\int_0^{2\pi} d\theta \xi \kappa^\beta \right) \kappa^{-\beta}$$

which significantly complicates the calculation.

When the cost function is written in terms of an integration over angle, by using $ds = \xi d\theta$, it has the form

$$C = \int_0^{2\pi} d\theta F(v, \kappa, \xi)$$

where all the dependence on the exponent β is contained in the velocity v . In general it is still very difficult (if not impossible) to minimize this cost function with respect to β exactly. It is therefore necessary to proceed with an approximation.

Consider the case of a circle: the curvature is a constant, independent of angle θ . By symmetry, the velocity must also be a constant, and hence this particular example is easy to solve. What can now be done is to consider shapes that are almost circular, for example ellipses with low eccentricity. These shapes are perturbations of the circular case, and therefore should be solvable up to some level of accuracy. It is now assumed that there exists some parameter ϵ that measures how close the shape in question is to a circle, for which $\epsilon = 0$. The curvature and differential ξ can be expanded in terms of this parameter

$$\kappa = \kappa_0 (1 + \epsilon \kappa_1 + \dots) \quad \xi = \xi_0 (1 + \epsilon \xi_1 + \dots)$$

where κ_0 and ξ_0 are the values for a circle and the higher order expansion terms, like κ_1 and ξ_1 , are angle dependent and specific to the shape in question. The method to be followed now is to substitute these expansions into the cost function and expand in a power series $\mathcal{C} = \mathcal{C}_0 + \mathcal{C}_1\epsilon + \mathcal{C}_2\epsilon^2 \dots$ where for example we have

$$\mathcal{C}_1 = \left. \frac{d\mathcal{C}}{d\epsilon} \right|_0 = \left. \frac{\partial F}{\partial v} \right|_0 \int_0^{2\pi} \left. \frac{dv}{d\epsilon} \right|_0 d\theta + \left. \frac{\partial F}{\partial \kappa} \right|_0 \int_0^{2\pi} \kappa_1 d\theta + \left. \frac{\partial F}{\partial \xi} \right|_0 \int_0^{2\pi} \xi_1 d\theta$$

with the notation $X|_0$ representing the quantity X evaluated for the circular case, i.e. with $\epsilon = 0$. To obtain the predicted exponent, this expansion must be minimized

$$\frac{d\mathcal{C}}{d\beta} = \frac{d\mathcal{C}_0}{d\beta} + \epsilon \frac{d\mathcal{C}_1}{d\beta} + \epsilon^2 \frac{d\mathcal{C}_2}{d\beta} \dots = 0. \quad (4)$$

Minimizing with respect to β at some order of perturbation theory will then give the exponent at that level of approximation. Clearly the first term of (4) is zero as this is simply the cost for a circle and must be independent of β . It can also be shown that \mathcal{C}_1 is also independent of β , and in fact the first contribution to (4) appears only at order ϵ^2 . Therefore the following must be solved

$$\epsilon^2 \frac{d}{d\beta} \mathcal{C}_2(\{\kappa_0, \xi_0, \kappa_1, \dots\}, \beta) = 0 \quad (5)$$

this requires a full evaluation of the integral \mathcal{C} keeping all terms at order ϵ^2 throughout. It should also be noted that because of the prefactor ϵ^2 in the equation above, the solution for the exponent will only be the zero-order term in an ϵ expansion for β . The accuracy of this value will be discussed later.

This is the method for calculating the exponent β . Because no values of the curvature or differential ξ have been specified, the derivation is quite general. After some algebra, the minimizing β can be found, and has the following value

$$\beta = \frac{10\overline{\Delta^2} + 5\eta^2\overline{\Delta'^2}}{15\overline{\Delta^2} + 15\eta^2\overline{\Delta'^2} + \eta^4\overline{\Delta''^2}} \quad (6)$$

where the various quantities have the following definition

$$\eta = (\kappa_0 \xi_0)^{-1} \quad \Delta = \kappa_1 - \bar{\kappa}_1 \\ X' = \frac{dX}{d\theta} \quad \bar{X} = \frac{1}{2\pi} \int_0^{2\pi} d\theta X(\theta)$$

and it should be noted that here X' means the derivative with respect to angle θ and that the exponent is a function of only $\{\kappa_0, \kappa_1, \xi_0\}$. The quantity η is unity for shapes that are deformation of a circle drawn once. However, it takes different values for more complex cases as will be shown below. The result is now examined for the drawing of two shapes that have appeared in the experimental literature: the ellipse and the cloverleaf.

3 The Ellipse

The most commonly used experimental task for analyzing the accuracy of the two-thirds power law is the drawing of ellipses of various sizes and eccentricity. This shape is therefore the obvious choice for testing the predictions of the minimum-jerk derived exponent with the experimentally accepted value of $1/3$. To calculate the exponent, the quantities $\{\kappa_0, \kappa_1, \xi_0\}$ specific to an almost-circular ellipse must be found. The following elliptical perturbation of a circle of unit radius will be used

$$x = \cos \theta \quad y = (1 - \epsilon)^{1/2} \sin \theta. \quad (7)$$

The arc-length differential of angle ξ and the curvature C are given by the standard formulae

$$\xi = \sqrt{\left(\frac{dx}{d\theta}\right)^2 + \left(\frac{dy}{d\theta}\right)^2} \quad \text{and} \quad \kappa = \frac{1}{\xi^3} \left(\left(\frac{dx}{d\theta}\right) \left(\frac{d^2y}{d\theta^2}\right) - \left(\frac{dy}{d\theta}\right) \left(\frac{d^2x}{d\theta^2}\right) \right)$$

and inserting the parametric equations (7) give the results

$$\begin{aligned} \xi &= (1 - \epsilon \cos^2 \theta)^{1/2} = 1 - \frac{\epsilon}{2} \cos^2 \theta + \dots \\ \kappa &= \frac{1}{\xi^3} (1 - \epsilon)^{1/2} = 1 + \frac{\epsilon}{2} (3 \cos^2 \theta - 1) + \dots \end{aligned}$$

The parameters required can be read off from the expansions above and inserted directly in the formulae necessary for calculating β given in the previous section. The final result for the exponent is

$$\beta = \frac{30}{91} = 0.3297 \quad (8)$$

which is remarkably close to the accepted value of $1/3$.

As stated previously, this result is only the first term in a perturbation series and its validity must be examined by obtaining the first correction. This can be done using a similar method to that described in the previous section but keeping all calculations up to a level of ϵ^4 . Calculation of the first correction yields the result

$$\beta = 0.32967 + 0.00034\epsilon^2.$$

The correction is quite small, and importantly implies that the leading order result (8) is actually valid for all ellipses that appeared in experiments. This derivation is a rigorous proof that the minimum-jerk model predicts an exponent equivalent to the empirical two-thirds power law for ellipses of all size, eccentricity and tracing period seen in experiment. It therefore generalizes and formalizes the similarity between coupled harmonic drawing and the minimum-jerk fit with four via-points, previously noted for the ellipse [13].

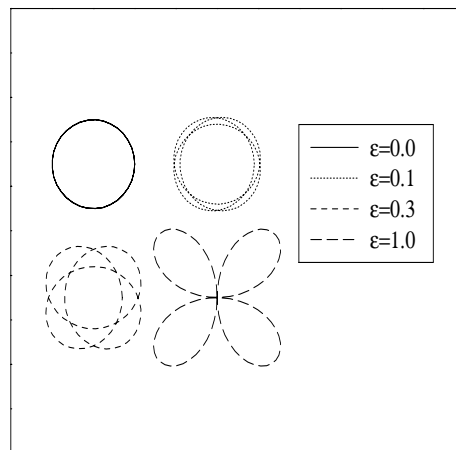


Fig. 1. Some examples of the generalized cloverleaf, as defined in the text. The forms for various values of the small parameter ϵ are given, with the value $\epsilon = 1$ corresponding to the shape used in experiment.

4 The Generalized Cloverleaf

In the previous section the case of an ellipse was analyzed. Though the choice of this shape is ubiquitous throughout the experimental literature it is, from the theoretical point of view, a special case. This is because the exact value of the exponent $1/3$ implies the simple motion of drawing with coupled harmonic motion (though it should be stressed that the exponent 0.3297 derived above implies more complex behavior). It is therefore worth examining

another shape that has also been measured in experiment: the cloverleaf. This is a more interesting shape than an ellipse, but shares the same property of a single segment on a $\log \kappa$ versus $\log v$ graph.

The form of the cloverleaf used in experiment is far removed from a circle. A more general form must be introduced that extrapolates between the two shapes. The following form is chosen here

$$x = \cos 3\theta(t) - \epsilon \cos \theta(t) \quad y = \sin 3\theta(t) + \epsilon \sin \theta(t) \quad (9)$$

and some examples for different values of ϵ are given in Fig. (1). For $\epsilon = 0$ the shape is circular by design, but it should be noted that the circle is traced three times, unlike in the elliptical case previously. The normal cloverleaf used in experiment takes the value $\epsilon = 1$. The important quantities in this case are

$$\begin{aligned} \xi &= (9 + 6\epsilon \cos 4\theta + \epsilon^2)^{1/2} \\ \kappa &= \frac{1}{\xi^3} (18 - 2\epsilon^2 + \xi^2). \end{aligned} \quad (10)$$

These formulae must again be expanded to find $\{\kappa_0, \kappa_1, \xi_0\}$. In this case the expansion gives $\xi_0 = 3$ as expected from the statement above concerning the three-cycled circle that is the basis for the perturbation. Inserting these forms in the general equation (6) predicts the following result for the cloverleaf

$$\beta = \frac{1530}{3631} = 0.4214. \quad (11)$$

Again, the validity of the approximation should be examined. In this case the correction is more significant

$$\beta = 0.4214 - 0.0017\epsilon^2.$$

This result is useful for generalized cloverleaves that are close to circles. Unfortunately $\epsilon = 1$, for the case of the experimentally used cloverleaf. Because of this, all orders ϵ^n will contribute equally. This means that the value derived by perturbation theory can only be used as a guide. Clearly it suggests that the exponent is larger than $1/3$. Interestingly, this is what is found in experiment for cloverleaves that are traced with periods of 2.5 and 3.0 seconds [4], where the average value of β was 0.353 and 0.360. (For completeness it should be noted that for faster tracing, with a period of 2 seconds, the value was lower $\beta = 0.325$, but this was due to a somewhat-anomalous data point.)

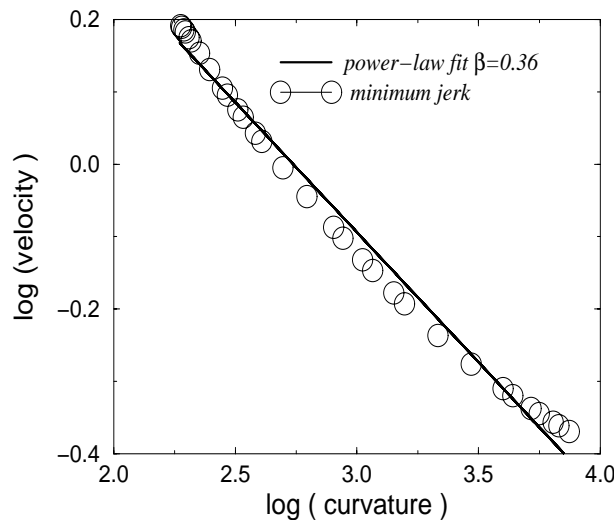


Fig. 2. The $\log(\text{curvature})$ versus $\log(\text{velocity})$ curve as was derived from the minimum-jerk cost function for a cloverleaf with $\epsilon = 1$. The value of the β exponent measured from this curve is $\beta = 0.36$, accurately reproducing the results found in experiment.

Though the value calculated above was shown only to be an approximation, a numerical method can be used to obtain the velocity profile from the minimum-jerk cost function (3) to an arbitrary degree of accuracy. Once the

velocity profile has been obtained the predicted exponent can be found from a least-squares fit of the relation (1): the approach used for experimental velocity curves. Such a velocity curve was obtained from (3), and the fit can be seen in Fig. (2). The exponent obtained was

$$\beta = 0.36 \pm 0.01 \quad (12)$$

which compares favorably with the experimental values given above. Though, due to the scatter seen in the experimental data, it would be too much to state that the minimum jerk result is better than the two-thirds power law prediction of $1/3$, the fact that this result is so accurate is indeed remarkable. It should be stressed here that this result cannot be dismissed as trivial (as has been done for the ellipse) by saying that it is a consequence of coupled harmonic motion: for the cloverleaf there are no coupled harmonic solutions. The result is therefore non-trivial and represents a surprising success of a first-principles approach for calculating the exponent, particularly since the only input into the theory is the curvature profile given by equations (9).

5 Summary and Conclusion

Two distinct motor control strategies, postulated to reflect some level of planning by the CNS, have been analyzed in mathematical detail with a view to provide a simple prescription for producing human-like movement by robots. One theory, the two-thirds power law, states that when the hand moves on a curved trajectory the velocity is proportional to a power of the local curvature. The second strategy, the minimum-jerk cost function, proposes that movements are generated by minimizing the time derivative of acceleration to produce smooth trajectories. By explicit calculation, it was shown that these apparently different theories produced common predictions. Two figural forms were analyzed: the ellipse and cloverleaf. The numerical values of the power-law exponents, were found to be $\beta = 0.33$ and $\beta = 0.36$ respectively, in remarkable agreement with experiment given the simple formulation of the minimum-jerk hypothesis. Taken with previous results for point-to-point movement [5] and the numerical results for more complex shapes [6], this suggests that the minimum-jerk cost function can be used to produce human-like movements for a wide variety of motor tasks performed in the plane commonly used for writing. This is not to say that it is closer to the planning strategies that the CNS is actually using - there exist more sophisticated proposals that capture subtle aspects of human movements that the minimum-jerk model misses [3, 8]. However, they are considerably more complex computationally, and in the context of mathematical simplicity the minimum-jerk cost-function approach is currently unrivaled in the breadth of experimental results that can be reproduced for movements in the plane.

6 Discussion

It terms of computational complexity, the two-thirds power law appears much easier to implement than the minimum-jerk hypothesis. This is because the former is a direct relation between velocity and curvature and the latter involves a minimizing-search through the space of possible curves. However, the power-law as it stands in equation (1) can only be used for very particular shapes, and worse still breaks down if a straight line or point of inflection is drawn. Moreover, the minimum-jerk hypothesis provides a full motion planning prescription that is significantly simpler than other similarly-versatile prescriptions. Nevertheless, it is well known that trajectories predicted by minimum jerk for three-dimensional movement do not match with experiment. The case of movement in three dimensions is considerably more complex than those in the plane, considered here. This is because planar movement described by an x and a y coordinate fixes to a large extent the joint angles at the shoulder and elbow. However, for movement in three dimensions, all seven degrees of freedom that the arm has are used. The hand's position and orientation does not contain enough information to fix all the arm's parameters, implying a "degrees of freedom" problem. Despite this added complexity, a number of studies have analyzed aspects of the arm's movement in three dimensions [15–17], though as yet, no comprehensive theory exists that captures all these aspects of motion. It should also be noted that hand and arm motion in three dimensions has been analyzed in the context of elliptical "waving" [18]. In this work, the recorded human-joint motion was implemented in an anthropomorphic robotic arm, and the results for the joint motion were found to be close to sinusoidal. However, for general three-dimensional motion a comprehensive theory is likely to be relatively complex given the number of degrees of freedom involved. Nevertheless, it represents an important theoretical aim, both for the fields of motor control and humanoid robotics.

References

1. Schaal, S. (1999). Is imitation learning the route to humanoid robots? *Trends in Cognitive Sciences* **3** 233-242.

2. Harris, C. M., (1998) On the optimal control of behaviour: a stochastic perspective . *Journal of Neuroscience Methods* **83** 73–88
3. Harris, C.M. and Wolpert, D. M. (1998) Signal-dependent noise determines motor planning. *Nature* **394** 780–784
4. Viviani, P. and Flash, T. (1995) Minimum-Jerk, Two-Thirds Power Law, and Isochrony: Converging Approaches to Movement Planning. *Journal of Experimental Psychology*, 21 32-53
5. Flash, T. and Hogan, N. (1985) The Coordination of Arm Movements: An Experimentally Confirmed Mathematical Model. *J. Neurosci.* **5** 1688–1703
6. Todorov, E. and Jordan, M. I. (1998) Smoothness Maximization Along a Predefined Path Accurately Predicts the Speed Profiles of Complex Arm Movements. *J. Neurophysiol.* **80**, 696-714
7. Desmurget, M., Jordan, M., Prablanc, C. and Jeannerod, M. Constrained and Unconstrained Movements Involve Different Control Strategies (1997) *J. Neurophys.* **77** 1644–1650
8. Uno, Y., Kawato, M. and Suzuki, R. (1989) Formation and control of optimal trajectories in human multijoint arm movements: Minimum torque-change model. *Biol. Cybern.* **61** 89–101
9. Viviani, P. and Cenzato, M. (1985) Segmentation and Coupling in Complex Movements. *Journal of Experimental Psychology*, 11 828-845
10. Viviani, P. and Schneider, R. (1991) Developmental Study of the Relationship Between Geometry and Kinematics in Drawing Movements. *Journal of Experimental Psychology*, 17, 198-218
11. de'Sperati, C. and Viviani, P. (1997) The Relationship between Curvature and Velocity in Two-Dimensional Smooth Pursuit Eye Movements. *Journal of Neuroscience*, 17 3932-3945
12. Lacquanti, F., Terzuolo, C. and Viviani, P. (1983) The law relating the kinematics and figural aspects of drawing movements. *Acta Psychologica*, 54 115-130
13. Wann, J., Nimmo-Smith, I. and Wing, A. M. (1988) Relation Between Velocity and Curvature in Movement: Equivalence and Divergence Between a Power Law and a Minimum-Jerk Model. *Journal of Experimental Psychology*, 14, 622-637
14. Viviani, P. (1986) Do Units of Motor Action Really Exist? *Experimental Brain Research Series* 15
15. Soechting, J., Buneo, C., Hermann, U., Flanders, M. (1995) Moving effortlessly in three dimensions: Does Donders' law apply to arm movement ? *Journal of Neuroscience* **15**, 6271–6280.
16. Gielen, C., Vrijenhoek, E.J., Flash, T., Neggers, S. (1997) Arm position constraints during pointing and reaching in 3-D space. *Journal of Neurophysiology* **78**, 660–673.
17. Vaughan J., Rosenbaum, D., Loukopoulos, L (1998) Finding final postures, *Journal of Motor Behavior* **30**, 273–284.
18. Sternad, D., Schaal, S. (1999) Segmentation of endpoint trajectories does not imply segmented control. *Exp. Brain Res.* **124**, 118–136.